ACS APPLIED BIO MATERIALS

www.acsabm.org Article

All-Natural Smart Mycelium Surface with Tunable Wettability

Wenjing Sun, Mehdi Tajvidi,* Christopher G. Hunt, and Caitlin Howell

Cite This: *ACS Appl. Bio Mater.* 2021, 4, 1015−1022 Read Online

ACCESS | Metrics & More | Article Recommendations | Supporting Information

ABSTRACT: A naturally occurring smart mycelium surface with tunable wettability is demonstrated. The commercially produced mycelium foam shows a natural hydrophobic and nonabsorbent surface with water contact angles well above 135°. The surface maintains its hydrophobicity and nonabsorbance after being compressed into a thin film under pressure and mild temperatures. We report that this surface carries tunable wettability. We have shown that a facile water treatment followed by room-temperature drying initially renders the surface highly hydrophilic and absorbent. Subsequent conditioning at 50 °C at any relative humidity turns the surface back to hydrophobic and partially restores nonabsorbance with a switchable character. We show that this change in surface wettability can be attributed to the increased water contact area and the surface hydroxyl groups of the fungal hyphae and the tunable property can be attributed to the presence of the surface amphiphilic protein, hydrophobin.

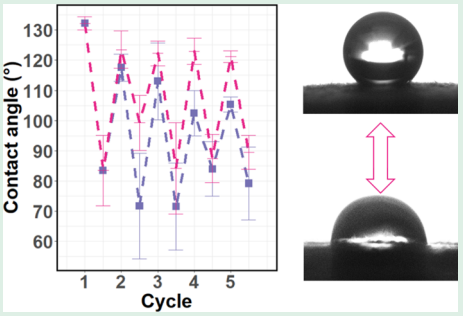

KEYWORDS: *mycelium, surface, wettability, hydrophobin, contact angle*

INTRODUCTION

Natural surfaces exhibit a variety of structures and chemical compositions which influence their wettability and absorbability. Some useful functionalities which exist in plant- or animal-based materials include superhydrophobic surfaces with self-cleaning properties,[1−3] superhydrophobic surfaces with high adhesive forces,[4] and patterned wetting for water collection,[5,6] among others. Learning from nature, artificial surfaces have been developed by fabricating hierarchical structures and applying chemical modifications afterward. These mimicked surfaces normally have similar functions to those naturally found but when they exhibit properties not found naturally, the practice is labeled "biomimicking beyond nature".[7] Surfaces with tunable wettability are an example of such types of artificial surfaces and have received broad scientific interest. Surface properties may be altered by diverse stimuli such as mechanical force, photoexposure, temperature change, pH change, electrical potential, electrolytes, and more.[8−10]

In addition to artificial smart surfaces, naturally existing biological systems can also exhibit the characteristics of self-healing and self-adjustment. For example, filamentous fungi can produce a type of surface amphiphilic protein called hydrophobin as a structural component. Hydrophobin proteins have relatively low molecular weight (about 100 amino acid residues) and are extractable with formic acid or trifluoroacetic acid.[11−13] They have both hydrophilic and hydrophobic parts to help fungi escape the aqueous environment to spread their spores by the self-assembly function.[14,15] The self-assembly property of hydrophobins under different conditions and environments has been widely investigated on extracted and purified hydrophobin proteins.[13,16−19] Specifically, the class I hydrophobin Vmh2 (0.1−0.2 mg mL^{-1} in 60% ethanol) extracted from the mycelium of oyster mushroom (*Pleurotus ostreatus*) undergoes a reversible conformational change from the helical structure to a disordered structure and reversible aggregation at a temperature of 80 °C.[19] Class I hydrophobin SC3 from the fungus *Schizophyllum commune* adopts the amyloid state at the water−PTFE interface at high concentration (300 $\mu g\ mL^{-1}$) and prolonged incubation (16 h).[18]

In recent years, fungal mycelium-based products have achieved increasing research interest and commercialization as novel sustainable materials to replace petroleum-based products. Specific products have been commercialized in textile, packaging, and construction applications.[20−22] In this work, we aim to understand the surface property of a commercialized mycelium product. Specifically, we were interested to know if the surface of mycelium carries switchable wettability similar to the exacted hydrophobin protein. We also further investigated the tunability of surface wettability and discussed possible mechanisms and potential applications.

Received: November 9, 2020
Accepted: December 15, 2020
Published: December 29, 2020

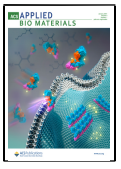

https://dx.doi.org/10.1021/acsabm.0c01449
ACS Appl. Bio Mater. 2021, 4, 1015−1022

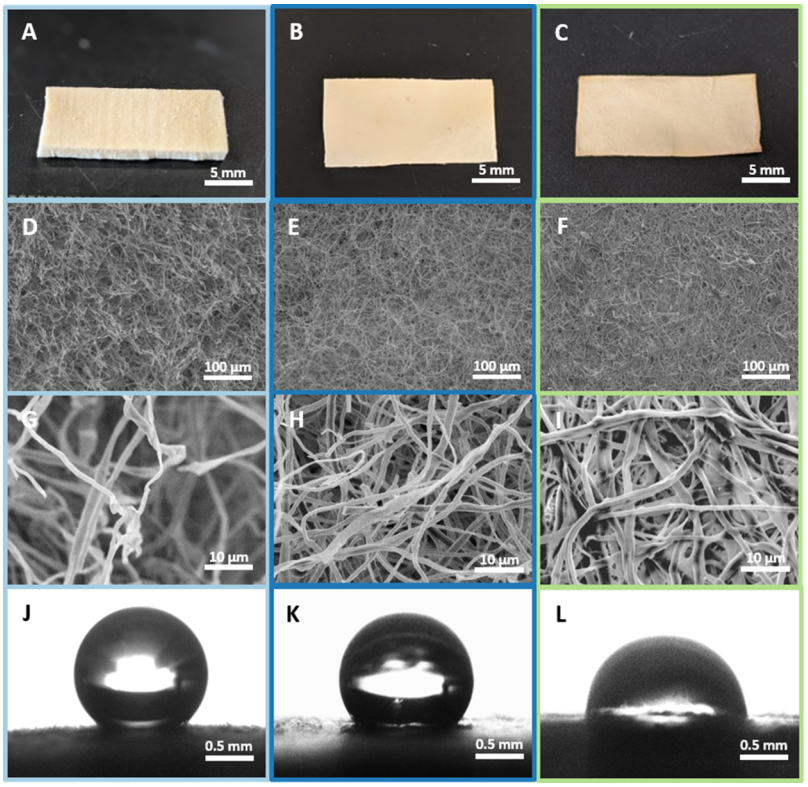

Figure 1. Morphology of MFoam (A,D,G), MFilm (B,E,H), and W/D MFilm (drying condition: 20 °C and 15 ± 5 % RH) (C,F,I). (A−C) Macroscale view. Scale bar: 5 mm. (D−F) SEM images of the microstructure. Scale bar: 100 μm. (G−I) SEM images of the microstructure. Scale bar: 10 μm. Initial contact angle image of MFoam (J), MFilm (K), and W/D MFilm (L). Scale bar: 0.5 mm.

MATERIALS AND METHODS

Sample Preparation. Ecovative Design, LLC, manufactured the pure mycelium sheet using a solid fermentation method, outlined elsewhere.[23] The obtained mycelium samples were cut into 20 × 10 × 2 mm sheets and labeled "MFoam" for further analysis. The "MFoam" was pressed under 5 MPa/80 °C for 5 min into "MFilm" with a thickness of about 0.15 (±0.02) mm.

We developed a facile water treatment method to change the wettability of the mycelium surface. To wet the mycelium surface, 100 μL of deionized water was applied on the surface of each mycelium film sample. A plastic blade was used to manually push water down with a horizontal back and forth motion into the mycelium structure until the entire mycelium film was fully saturated with water. The samples were dried and conditioned on the laboratory bench in open air at a temperature of 20 ± 1 °C and a relative humidity (RH) of 15 ± 5 % until no weight change was recorded. The resulting wetted/dried samples are labeled "W/D MFilm".

To remove the surface hydrophobins of the MFilm, the samples were saturated with 99% formic acid at 4 °C for 24 h according to previous reports[11,24] and then washed with distilled water until the pH reached 7 and dried under laboratory condition until no weight change was observed.

Conditioning Treatment. The wetted and redried mycelium films were conditioned for up to 13 days. The four conditions were 50 °C and 80% RH; 50 °C and 3% RH; 20 °C and 80% RH; and 20 °C and 50% RH. At the end of the conditioning treatments, the samples were placed in the laboratory until no weight change was observed.

Scanning Electron Microscopy. The morphology of the mycelium surface was investigated by scanning electron microscopy (SEM) (Amray 1820, Amray Inc., New Bedford, MA, USA). The surface of the samples was coated with gold (3 nm) before observation at 10 kV acceleration voltage on various locations and at ×200 and ×2000 magnifications.

Contact Angle and Wetting Time Measurement. The contact angle analysis was carried out using a mobile contact angle analyzer (KRÜSS GmbH, MSA, Hamburg, Germany) and the corresponding software for this device. For each measurement, one 1 μL drop of water was applied on a random area of the surface, and the time series of contact angles were collected starting at an average 2.5 ± 0.5 s after the start of the experiment until total absorption or evaporation. For all analyses, the initial contact angles were determined at 2.5 ± 0.5 s by averaging left and right side angles of the droplets. For each sample, 5−15 measurements were carried out.

Light Microscopy. A Nikon NIE microscope (Nikon Instruments Inc., Melville, NY) was used to image the samples and obtain z-stack images (bright-field). The objective lens was a Nikon Plan Fluor 40× PH2 DLL, with a numerical aperture (NA) of 0.75 and a depth-of-field of 0.98 μm.

Moisture Content Analysis. Thermogravimetric analysis was used to measure the moisture content of MFilm and W/D MFilm under nitrogen gas on a TGA Q500 (TA Instruments, New Castle, DE). The TGA temperature was increased from room temperature to 110 °C at a rate of 20 °C min^{-1} and then held at 110 °C for 20 min. The moisture content was calculated based on the mass loss detected by TGA.

Thermogravimetric Analysis. The thermal stability evaluation of the materials was carried out under nitrogen gas on a TGA Q500 (TA Instruments, New Castle, DE) with a high-resolution (Hi-Res) option to differentiate overlapping decomposition peaks. In the Hi-Res approach, the temperature range is from room temperature to 600 °C. The heating rate is dynamically and continuously modified, ranging from 0.001 °C min^{-1} to the maximum heating rate (20 °C min^{-1}) in response to changes in the decomposition rate of the sample. The resolution and sensitivity settings were 4.0 and 1.0 °C, respectively. The TGA results are shown as the variation of the sample mass (TG) or as a derivative weight loss (DTG) curve corresponding to the temperature.

Attenuated Total Reflectance−Fourier Transform Infrared Spectroscopy. Attenuated total reflectance−Fourier transform infrared (ATR−FTIR) spectra of the surface were obtained using a

https://dx.doi.org/10.1021/acsabm.0c01449
ACS Appl. Bio Mater. 2021, 4, 1015−1022

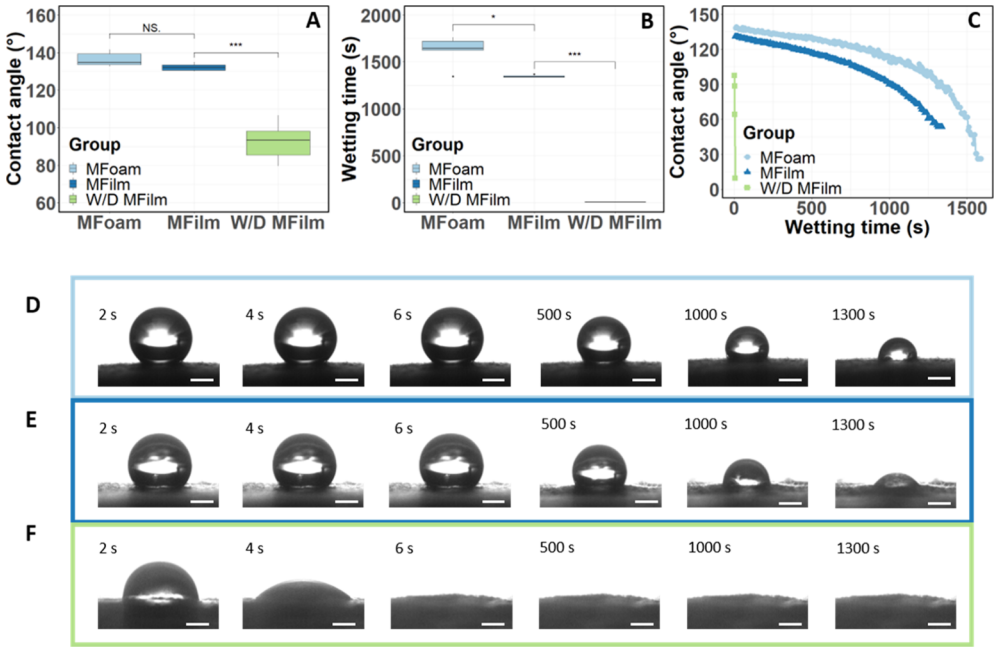

Figure 2. Wettability and absorption comparison of MFoam, MFilm, and W/D MFilm (drying condition: 20 °C and 15 ± 5 % RH). (A) Initial contact angle (deg). (B) Wetting time (s). (NS indicates $p > 0.05$; * indicates $p < 0.05$; and *** indicates $p < 0.001$) (C) Change in the contact angle with wetting time: MFoam (D), MFilm (E), and W/D MFilm (F). Scale bar: 0.5 mm.

Spectrum Two IR spectrometer (PerkinElmer, Waltham, MA). All spectra were obtained in the range of 4000−500 cm^{-1}, accumulating 32 scans. The tested samples were all under room condition. To ensure the reproducibility of the obtained spectra, three replicate specimens were measured.

RESULTS AND DISCUSSION

Surface Wettability. Figure 1A shows the original mycelium foam (MFoam) produced by Ecovative Design, LLC (Green Island, NY). Visual inspection of the SEM image (Figure 1D) shows that the distribution of the hyphae is uniform. The 2 mm-thick MFoam was compressed to about 0.15 (±0.02) mm (Figure 1B) in thickness. The compression is visible when comparing the MFoam with the MFilm at moderate (Figure 1D,E) and high (Figure 1G,H) magnification (×2000). The compression process maintains the hydrophobicity of the original foam. As shown in Figure 2A, there is no significant difference ($p > 0.05$) between the initial water contact angle of the original MFoam and the compressed MFilm (135 ± 4 vs 130 ± 2°, respectively). The hydrophobic nature of filamentous fungi is well-known and is attributed to assemblies of the surface-active protein, hydrophobin.[12,17,25] Furthermore, as shown in Figure 2C,D, with the increase in the wetting time, the single water droplet on the surface of MFoam undergoes a typical three-stage route: (1) reduced contact angle; (2) reduced contact line with small contact angle changes; and (3) a mixed mode of 1 and 2[26] and finally disappears after about 1600 s (Figure 2B−D). This behavior is similar to the behavior of common hydrophobic or nearly hydrophobic surfaces.[26] There is also no detectable weight change after the water droplet disappears, indicating that the applied water droplet mostly evaporated without being absorbed into the porous structure. The compressed film showed a similar trend but with shorter wetting time (Figure 2B,C,E). This behavior could be attributed to partial water penetration between the hyphae. We also performed the wetting test on a nonabsorbing Teflon surface as a reference. The contact angle and wetting time were 102 ± 5° and 1127 ± 144 s, respectively. The wetting time (actually evaporation time) on the Teflon sheet was significantly less ($p < 0.05$) than MFilm and MFoam, which may be due to the larger surface area of the same drop volume on Teflon.[27]

To further investigate the absorption behavior and the amphiphilicity of the mycelium surface, 100 μL (per 200 mm^2 area of mycelium) of water was applied to each MFilm sample and pressed into the surface to accelerate the absorption. The applied water was eventually absorbed, with water displacing internal air pockets evidenced by a change from white to a slightly translucent appearance. After drying at room temperature (20 ± 1 °C) and humidity (15 ± 5 % RH), a film with a denser surface was obtained (Figure 1C,F,I). The smaller opening area is caused by the apparent additional connectivity among hyphae (Figure 1F,I). The wettability of the wetted/dried mycelium film also changed significantly ($p < 0.001$) with the initial contact angle dropping to 93 ± 9° (Figure 2A) and the total wetting time reduced to less than 10 s (8 ± 2 s) (Figure 2B,C,F). This dramatic change in the wettability and absorption of W/D MFilm could be caused by the change in the physical surface structure such as the reduced amount of air pockets and/or by the chemical surface components such as the reassembly of the surface hydrophobin proteins or a combination of these two factors.

MFilm Versus W/D MFilm. Comparing the SEM images of MFilm and W/D MFilm shows that once the MFilm is wetted and redried (Figure 1C,F,I), the mat structure does not appear to alter, but there appears to be material bridging hyphae at many intersections (fillets), which would suggest additional bonding between hyphae (Figure 1H vs 1I). To further investigate the changes happening at different depths from the surface, we prepared a series of z-stack light microscopy images of MFoam, MFilm, and W/D MFilm (Figure 3A−C). In this figure, the numbers from 1 to 7 indicate the images taken from the first visible hypha on the

https://dx.doi.org/10.1021/acsabm.0c01449
ACS Appl. Bio Mater. 2021, 4, 1015−1022

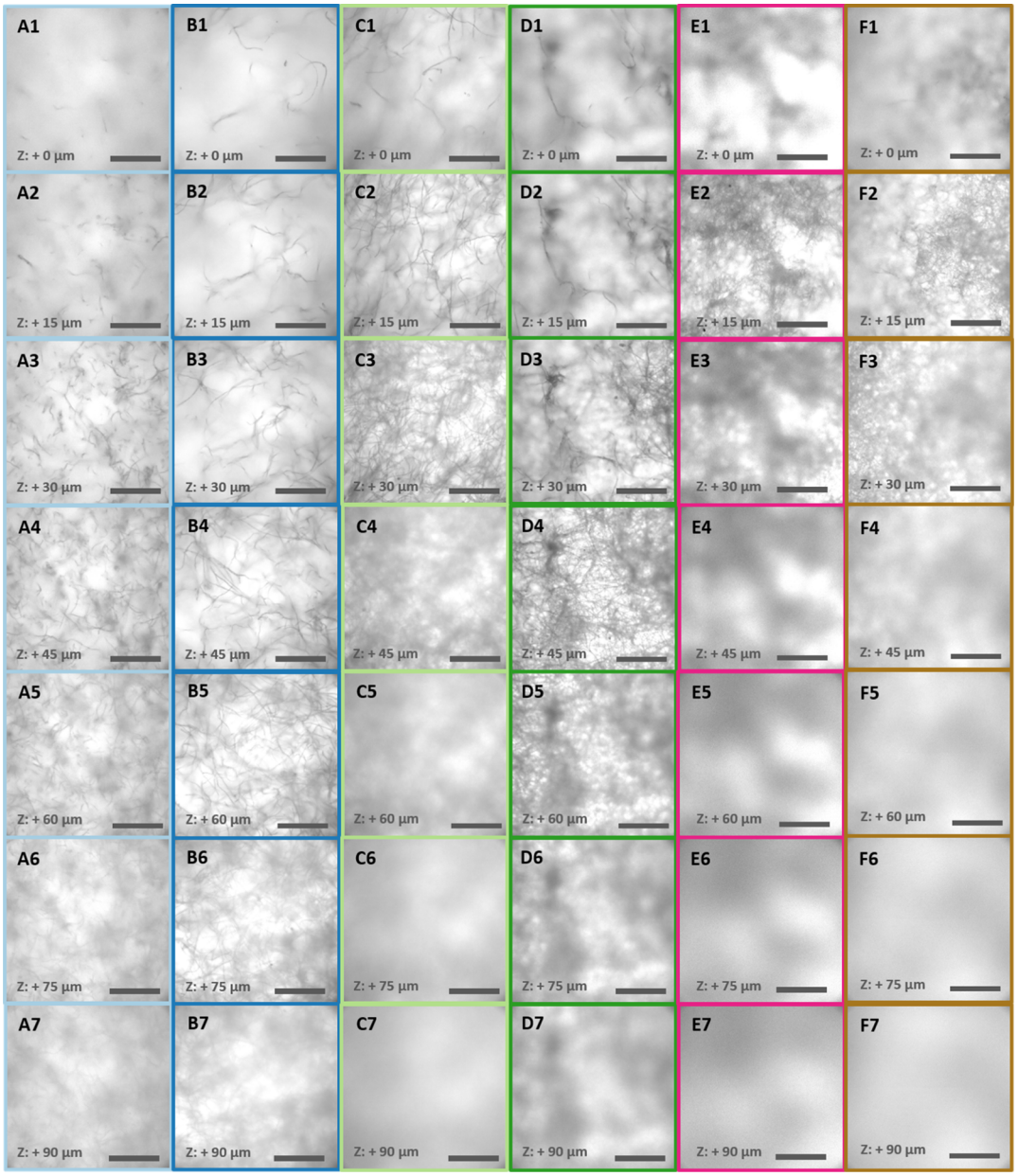

Figure 3. Z-stack images of (A) MFoam, (B) MFilm, (C) W/D MFilm (drying condition: 20 °C and 15 ± 5 % RH), (D) acid-treated MFilm, (E) W/D MFilm after conditioning (50 °C and 80% RH) for 15 days, and (F) acid-treated film after conditioning (50 °C and 80% RH) for 15 days. Scale bar: 100 μm.

surface down to 90 μm depth at 15 μm intervals. For MFoam and MFilm, the individual hyphae were clear and distinct up to Figure 3 A6 and B6, whereas for W/D MFilm, there was no distinct hyphae observed in Figure 3 C4. Therefore, the densification of the surface and the swelling of hyphae may attribute the change in wettability and surface hydrophobicity.

Changes in surface morphology and arrangements of chemical components of W/D MFilm may also trap more water molecules in the structure and thus influence the wettability. To measure the potential small changes in moisture content, thermogravimetric analysis was applied on MFilm and W/D MFilm conditioned at the same room temperature and humidity (20 ± 1 °C and 15 ± 5% RH). As shown in Table 1, the moisture content of both MFilm and W/D MFilm was both about 10% and there was no significant difference (p > 0.05) between the moisture contents of the two films.

Table 1. Moisture Content (%) Determined by Thermogravimetric Analysis and OH/CO Ratio Determined by ATR−FTIR of MFilm and W/D MFilm

groups	MFilm	W/D MFilm
moisture content (%)	10.1 (±2.31)	10.2 (±0.97)
OH/CO ratio	0.18 (±0.01)	0.20 (±0.00)

Considering the fact that the total moisture content may not fully represent the mycelium surface, we also calculated the ratio of O−H and C−O groups on the surface spectra curve obtained from ATR−FTIR analysis. The OH/CO ratio of W/D MFilm was 0.02 (11%) higher than the ratio in the MFilm, indicating that there was a potential increase in available hydroxyl groups, which may contribute to the increased wetting.

https://dx.doi.org/10.1021/acsabm.0c01449
ACS Appl. Bio Mater. 2021, 4, 1015−1022

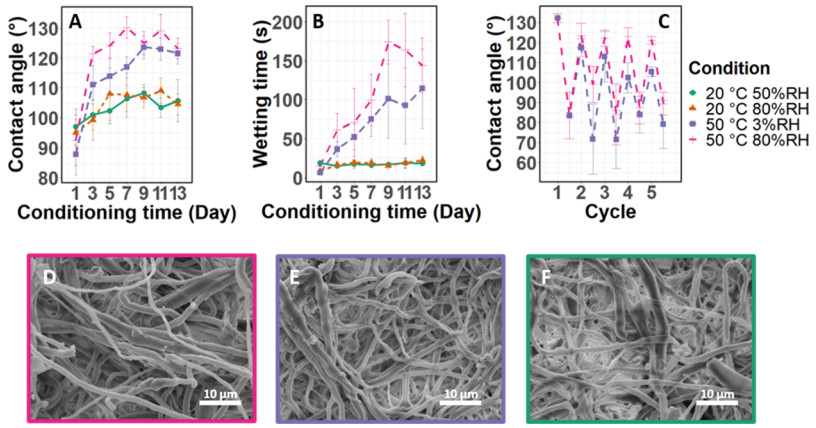

Figure 4. Changes in W/D MFilm (A) contact angle and (B) wetting/absorption time, with conditioning time. Window (C) shows the switch of wettability after multiple wetting and conditioning cycles; SEM images of W/D MFilm after conditioning for 15 days at (D) 50 °C and 80% RH, (E) 50 °C and 3% RH, and (F) 20 °C and 50% RH are also presented. Scale bar: 10 μm.

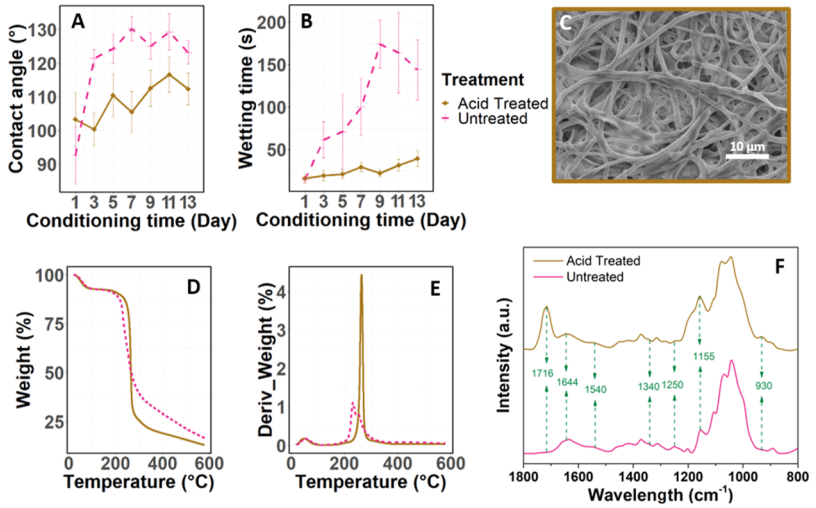

Figure 5. Influence of (A) acid treatment on the contact angle and (B) wetting time after conditioning at 50 °C and 80% RH C: SEM image of the acid-treated film surface. Scale bar: 10 μm. (D) TG, (E) DTG, and (F) FTIR curves of untreated and acid-treated MFilm.

Tunability of Wetting/Absorption. To evaluate potential surface chemistry changes influencing wettability, we further designed conditioning tests to understand if the surface wettability would change when the surface is exposed to higher temperature and/or humidity conditions. Comparisons of the wettability of the wetted/redried mycelium film exposed to different temperatures and relative humidity, as measured by the change in contact angle and total wetting time under laboratory conditions, are presented in Figure 4. As shown in Figure 4A,B, temperature has a noticeable effect on both the contact angle and wetting time of the MFilm. The two groups that were conditioned at 20 °C both showed a noticeably lower contact angle and wetting time (Figure 4A,B). When conditioning at high temperature (50 °C), the initial contact angle returned to >120° after 3 days for high (80%) RH or 9 days at low (3%) RH and remained stable afterward. However, for the two groups that were conditioned at room temperature, the contact angle only returned to ∼110°. The wetting time showed a similar trend as well. At high humidity, the conditioning treatment performance was better, which might be explained by the plasticization effect of water on the material matrix allowing rearrangement of amphiphilic hydrophobin molecules back to their original prewetting condition. Figure 4D,E,F shows the surface morphology of the wetted mycelium film after being conditioned for 15 days under 50 °C and 80% RH, 50 °C and 3% RH, and 20 °C and 50% RH, respectively. Compared with Figure 1I, the swelling of hyphae remains similar in both groups. The distance between different layers of hyphae is not clear in the SEM images, but from the z-stack images shown in Figure 3C,E, there are no noticeable changes in the z-distance of the W/D MFilm before and after conditioning. Additionally, although the high-temperature conditioning was able to reverse the wettability of the mycelium surface, wetting/absorption time (Figure 3B) was still 10 times faster than the original mycelium films (Figure 2B), which could be explained by the increase in the surface in contact with the water droplet.

To test the tunability of the MFilm surface properties, the wetting and conditioning processes (3 days in total) were repeated for five cycles. The changes in contact angles are shown in Figure 4C, confirming the consistent switching of wettability over five cycles. It can be seen that regardless of conditioning treatment applied, the high initial contact angles can be restored by conditioning even after five cycles of wetting/redrying/conditioning.

https://dx.doi.org/10.1021/acsabm.0c01449
ACS Appl. Bio Mater. 2021, 4, 1015−1022

Role of Hydrophobins. To further confirm that hydrophobins were indeed the cause of the observed switchable hydrophobicity, we treated the MFilm with formic acid to extract the hydrophobin proteins. We used very low temperature (4 °C) to minimize changes to other structural components. The wettability of the MFilm before and after formic acid treatment were compared and are shown in Figure 5A,B. Formic acid-washed W/D MFilms lost their ability to become hydrophobic again after conditioning (Figure 5B), a result consistent with the proposed hydrophobin mechanism of switchable hydrophobicity. Figure 5C shows the SEM image of acid-treated MFilm. The morphology is quite similar compared with that of the W/D film. The z-stack image series suggests that densification is slightly lower than that of the W/D MFilm but more than the MFilm (Figure 3D) and that there is not much difference in *z*-distance of the acid-treated film after conditioning compared with the W/D film (Figure 3F).

TGA and ATR−FTIR were carried out on the untreated and acid-treated MFilms to reveal if there are corresponding changes in the chemical component. In the ATR−FTIR curves shown in Figure 5F (the full spectrum is provided in Figure S1), the amide I (1644 cm^{-1}) and amide II (1540 cm^{-1}) peaks, which are attributed to C═O stretching and N−H bending,[28] do not show a marked difference compared to the untreated MFilm. The peak at 1340 and 1250 cm^{-1} in the amide III region attributed to C−N stretching and N−H bending decreased remarkably, which may relate to the partial removal of surface hydrophobins. The peak at 1716 cm^{-1} representing C═O stretching showed up in the acid-treated sample, which may have been caused by the residual formic acid in the structure.[29] The peak at 1155 cm^{-1} corresponding to the stretching of C−O is much higher in acid-treated samples than in the untreated sample; this may indicate more exposed polysaccharides. This could also be confirmed by the presence of the peak at 930 cm^{-1} which represents the vibration of the C−O−C bridge.[30]

The Hi-Res option of TGA is often used to differentiate overlapping or close decomposition peaks. As shown in the DTG curve (Figure 5E), two peaks appearing at 231 and 250 °C were separated in the curve of untreated MFilm, whereas there was only one peak shown in the acid-treated MFilm. The disappearance of one peak indicates that the amount of one component in the MFilm has notably decreased after acid treatment. In the TG curve (Figure 5D), the acid-treated MFilm showed less residue after 600 °C, which may have been caused by the release of acidic species catalyzing the dehydration of carbohydrates to produce more thermally stable char.[31]

Potential Applications. The switchable wetting properties of this commercially available natural material have the potential to be used in many applied areas. Figure 6 shows two possible applications. The first application is patterning on MFilm (Figure 6A). In this example, the background of the letters was masked by an adhesive tape where the areas covered by letters were treated with water. The wettability of the area of the letters changed from hydrophobic to hydrophilic by applying water (Figure 6A1) and room-temperature drying (Figure 6A2). When a water-based dye is applied to the surface, the original pattern appears (Figure 6A3).

Figure 6B reveals the potential utilization of the MFilm in microfluidic-related applications. After treating the designed channel with water and letting it dry at room temperature, the channel becomes hydrophilic while other background areas remain hydrophobic. The applied drop of water then moves back and forth across the film following the channel. One issue for this application is that once the surface becomes hydrophilic, it also becomes absorbing. In this example, the water drop was partially absorbed and lost its original volume once it passed through the channel. Further modification and designs are needed to overcome this issue.

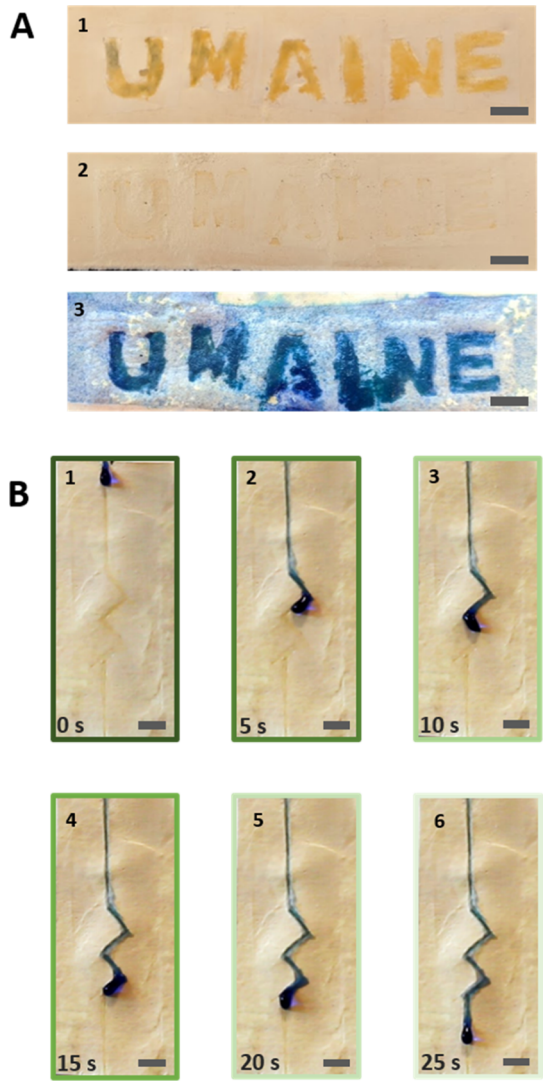

Figure 6. (A) Patterning process of MFilm. The area not covered by UMAINE letters was masked by an adhesive tape before water treatment. (B) Potential microfluidic channel application. Scale bar: 5 mm.

Apart from potential applications, considering the similarities of the hydrophobicity of aerial mycelium of different species of basidiomycete fungi, we also conducted similar tests on the mycelium of a known fungal species (*Trametes versicolor*) grown in the laboratory. We obtained very similar results of the switchable wetting properties (shown in Supporting Information Table S1, Figure S2, and Figure S3). Therefore, we can expect that this tunable wettability may be common within the basidiomycete family and more fungal species can be investigated in future to identify appropriate species or strains of fungus for specific applications.

https://dx.doi.org/10.1021/acsabm.0c01449
ACS Appl. Bio Mater. 2021, 4, 1015−1022

CONCLUSIONS

We have demonstrated a simple method to alter surface properties of a commercially available mycelium material that can be used to produce all-natural surfaces with reversible wettability. Surfaces can be made hydrophilic by forced wetting or prolonged water exposure and hydrophobic by exposure to temperatures up to 50 °C. The rearrangement of the amphiphilic protein hydrophobin was identified as the potential mechanism behind the behavior. Our findings suggest a possible low-cost and all-natural resource for multiple applications in different fields, such as microfluidics, smart coatings, and self-cleaning surfaces.

ASSOCIATED CONTENT

Supporting Information

The Supporting Information is available free of charge at https://pubs.acs.org/doi/10.1021/acsabm.0c01449.

Full FTIR spectra of untreated and acid-treated MFilm presented in Figure 5, contact angle and moisture content comparison of *T.vers* MFilm and W/D MFilm, change in contact angle and wetting/absorption time with conditioning time, and influence of acid treatment for *T.vers* W/D MFilm (PDF)

AUTHOR INFORMATION

Corresponding Author

Mehdi Tajvidi − *Laboratory of Renewable Nanomaterials, School of Forest Resources, University of Maine, Orono, Maine 04469-5755, United States; Advanced Structures and Composites Center, University of Maine, Orono, Maine 04469-5755, United States;* orcid.org/0000-0002-3549-1220; Email: mehdi.tajvidi@maine.edu

Authors

Wenjing Sun − *Laboratory of Renewable Nanomaterials, School of Forest Resources, University of Maine, Orono, Maine 04469-5755, United States; Advanced Structures and Composites Center, University of Maine, Orono, Maine 04469-5755, United States;* orcid.org/0000-0002-8850-6713

Christopher G. Hunt − *USDA Forest Products Laboratory, Madison, Wisconsin 53726, United States;* orcid.org/0000-0002-4799-7085

Caitlin Howell − *Department of Chemical and Biomedical Engineering and Graduate School of Biomedical Science and Engineering, University of Maine, Orono, Maine 04469-5755, United States;* orcid.org/0000-0002-9345-6642

Complete contact information is available at: https://pubs.acs.org/10.1021/acsabm.0c01449

Author Contributions

The manuscript was written through contributions of all authors. All authors have given approval to the final version of the manuscript.

Notes

The authors declare no competing financial interest.

ACKNOWLEDGMENTS

The authors thank Ecovative Design, LLC for providing the raw materials. This work is supported by the U.S. Department of Agriculture's Agricultural Research Service (USDA ARS Agreement no. 58-0204-003).

ABBREVIATIONS

DTG, the derivative weight loss; RH, relative humidity; SEM, scanning electron microscopy; TG, the variation of the sample mass; TGA, thermogravimetric analysis; ATR−FTIR, attenuated total reflectance−Fourier transform infrared

REFERENCES

(1) Neinhuis, C.; Barthlott, W. Characterization and distribution of water-repellent, self-cleaning plant surfaces. *Ann. Bot.* **1997**, *79*, 667−677.

(2) Barthlott, W.; Neinhuis, C. Purity of the sacred lotus, or escape from contamination in biological surfaces. *Planta* **1997**, *202*, 1−8.

(3) Guo, Z.; Liu, W. Biomimic from the superhydrophobic plant leaves in nature: Binary structure and unitary structure. *Plant Sci.* **2007**, *172*, 1103−1112.

(4) Zheng, Y.; Gao, X.; Jiang, L. Directional adhesion of superhydrophobic butterfly wings. *Soft Matter* **2007**, *3*, 178−182.

(5) Hu, D. L.; Chan, B.; Bush, J. W. M. The hydrodynamics of water strider locomotion. *Nature* **2003**, *424*, 663−666.

(6) Zheng, Y.; Bai, H.; Huang, Z.; Tian, X.; Nie, F.-Q.; Zhao, Y.; Zhai, J.; Jiang, L. Directional water collection on wetted spider silk. *Nature* **2010**, *463*, 640−643.

(7) Liu, X.; Liang, Y.; Zhou, F.; Liu, W. Extreme wettability and tunable adhesion: biomimicking beyond nature? *Soft Matter* **2012**, *8*, 2070−2086.

(8) Xia, F.; Zhu, Y.; Feng, L.; Jiang, L. Smart responsive surfaces switching reversibly between super-hydrophobicity and super-hydrophilicity. *Soft Matter* **2009**, *5*, 275−281.

(9) Stratakis, E.; Mateescu, A.; Barberoglou, M.; Vamvakaki, M.; Fotakis, C.; Anastasiadis, S. H. From superhydrophobicity and water repellency to superhydrophilicity: smart polymer-functionalized surfaces. *Chem. Commun.* **2010**, *46*, 4136−4138.

(10) Guo, F.; Guo, Z. Inspired smart materials with external stimuli responsive wettability: a review. *RSC Adv.* **2016**, *6*, 36623−36641.

(11) Wessels, J.; De Vries, O.; Asgeirsdottir, S. A.; Schuren, F. Hydrophobin genes involved in formation of aerial hyphae and fruit bodies in *Schizophyllum*. *Plant Cell* **1991**, *3*, 793−799.

(12) Bidochka, M. J.; St Leger, R. J.; Joshi, L.; Roberts, D. W. The rodlet layer from aerial and submerged conidia of the entomopathogenic fungus *Beauveria bassiana* contains hydrophobin. *Mycol. Res.* **1995**, *99*, 403−406.

(13) Lo, V.; Ren, Q.; Pham, C.; Morris, V.; Kwan, A.; Sunde, M. Fungal hydrophobin proteins produce self-assembling protein films with diverse structure and chemical stability. *Nanomaterials* **2014**, *4*, 827−843.

(14) Linder, M. B.; Szilvay, G. R.; Nakari-Setälä, T.; Penttilä, M. E. Hydrophobins: the protein-amphiphiles of filamentous fungi. *FEMS Microbiol. Rev.* **2005**, *29*, 877−896.

(15) Kershaw, M. J.; Talbot, N. J. Hydrophobins and repellents: proteins with fundamental roles in fungal morphogenesis. *Fungal Genet. Biol.* **1998**, *23*, 18−33.

(16) Armenante, A.; Longobardi, S.; Rea, I.; De Stefano, L.; Giocondo, M.; Silipo, A.; Molinaro, A.; Giardina, P. The *Pleurotus ostreatus* hydrophobin Vmh2 and its interaction with glucans. *Glycobiology* **2010**, *20*, 594−602.

(17) Aimanianda, V.; Bayry, J.; Bozza, S.; Kniemeyer, O.; Perruccio, K.; Elluru, S. R.; Clavaud, C.; Paris, S.; Brakhage, A. A.; Kaveri, S. V.; Romani, L.; Latgé, J.-P. Surface hydrophobin prevents immune recognition of airborne fungal spores. *Nature* **2009**, *460*, 1117−1121.

(18) Scholtmeijer, K.; de Vocht, M. L.; Rink, R.; Robillard, G. T.; Wösten, H. A. B. Assembly of the fungal SC3 hydrophobin into functional amyloid fibrils depends on its concentration and is promoted by cell wall polysaccharides. *J. Biol. Chem.* **2009**, *284*, 26309−26314.

(19) Longobardi, S.; Picone, D.; Ercole, C.; Spadaccini, R.; Stefano, L. D.; Rea, I.; Giardina, P. Environmental conditions modulate the switch among different states of the hydrophobin Vmh2 from *Pleurotus ostreatus*. *Biomacromolecules* **2012**, *13*, 743−750.
(20) Sun, W.; Tajvidi, M.; Hunt, C. G.; McIntyre, G.; Gardner, D. J. Fully bio-based hybrid composites made of wood, fungal mycelium and cellulose nanofibrils. *Sci. Rep.* **2019**, *9*, 1−12.
(21) Appels, F. V. W.; Camere, S.; Montalti, M.; Karana, E.; Jansen, K. M. B.; Dijksterhuis, J.; Krijgsheld, P.; Wösten, H. A. B. Fabrication factors influencing mechanical, moisture-and water-related properties of mycelium-based composites. *Mater. Des.* **2019**, *161*, 64−71.
(22) Attias, N.; Danai, O.; Abitbol, T.; Tarazi, E.; Ezov, N.; Pereman, I.; Grobman, Y. J. Mycelium bio-composites in industrial design and architecture: Comparative review and experimental analysis. *J. Cleaner Prod.* **2020**, *246*, 119037.
(23) Islam, M. R.; Tudryn, G.; Bucinell, R.; Schadler, L.; Picu, R. C. Morphology and mechanics of fungal mycelium. *Sci. Rep.* **2017**, *7*, 13070.
(24) de Vries, O. M. H.; Fekkes, M. P.; Wösten, H. A. B.; Wessels, J. G. H. Insoluble hydrophobin complexes in the walls of Schizophyllum commune and other filamentous fungi. *Arch. Microbiol.* **1993**, *159*, 330−335.
(25) Gunning, A. P.; De Groot, P. W. J.; Visser, J.; Morris, V. J. Atomic force microscopy of a hydrophobin protein from the edible mushroom *Agaricus bisporus*. *J. Colloid Interface Sci.* **1998**, *201*, 118−126.
(26) Park, J. K.; Ryu, J.; Koo, B. C.; Lee, S.; Kang, K. H. How the change of contact angle occurs for an evaporating droplet: effect of impurity and attached water films. *Soft Matter* **2012**, *8*, 11889−11896.
(27) Chandra, S.; di Marzo, M.; Qiao, Y. M.; Tartarini, P. Effect of liquid-solid contact angle on droplet evaporation. *Fire Saf. J.* **1996**, *27*, 141−158.
(28) Lecellier, A.; Mounier, J.; Gaydou, V.; Castrec, L.; Barbier, G.; Ablain, W.; Manfait, M.; Toubas, D.; Sockalingum, G. D. Differentiation and identification of filamentous fungi by high-throughput FTIR spectroscopic analysis of mycelia. *Int. J. Food Microbiol.* **2014**, *168*−*169*, 32−41.
(29) Zhang, M.; Qi, W.; Liu, R.; Su, R.; Wu, S.; He, Z. Fractionating lignocellulose by formic acid: Characterization of major components. *Biomass Bioenergy* **2010**, *34*, 525−532.
(30) Fernando, I. P. S.; Sanjeewa, K. K. A.; Samarakoon, K. W.; Lee, W. W.; Kim, H.-S.; Kim, E.-A.; Gunasekara, U. K. D. S. S.; Abeytunga, D. T. U.; Nanayakkara, C.; De Silva, E. D.; Lee, H.-S.; Jeon, Y.-J. FTIR characterization and antioxidant activity of water soluble crude polysaccharides of Sri Lankan marine algae. *Algae* **2017**, *32*, 75−86.
(31) Alongi, J.; Carletto, R. A.; Bosco, F.; Carosio, F.; Di Blasio, A.; Cuttica, F.; Antonucci, V.; Giordano, M.; Malucelli, G. Caseins and hydrophobins as novel green flame retardants for cotton fabrics. *Polym. Degrad. Stab.* **2014**, *99*, 111−117.

https://dx.doi.org/10.1021/acsabm.0c01449
ACS Appl. Bio Mater. 2021, 4, 1015−1022

Supporting information

All-natural Smart Mycelium Surface with Tunable Wettability

Wenjing Sun[1,2], Mehdi Tajvidi[1,2], Christopher G. Hunt[3], and Caitlin Howell[4,5]*

[1]Laboratory of Renewable Nanomaterials, School of Forest Resources, University of Maine, Nutting Hall, Orono, ME 04469-5755, USA

[2]Advanced Structures and Composites Center, University of Maine, 35 Flagstaff Road, Orono, ME 04469-5755, USA

[3]USDA Forest Products Laboratory, 1 Gifford Pinchot Drive, Madison, WI, 53726, USA

[4]Department of Chemical and Biomedical Engineering, University of Maine, Orono, Maine 04469-5755, USA

[5]Graduate School of Biomedical Science and Engineering, University of Maine, Orono, Maine 04469-5755, USA

Email: mehdi.tajvidi@maine.edu

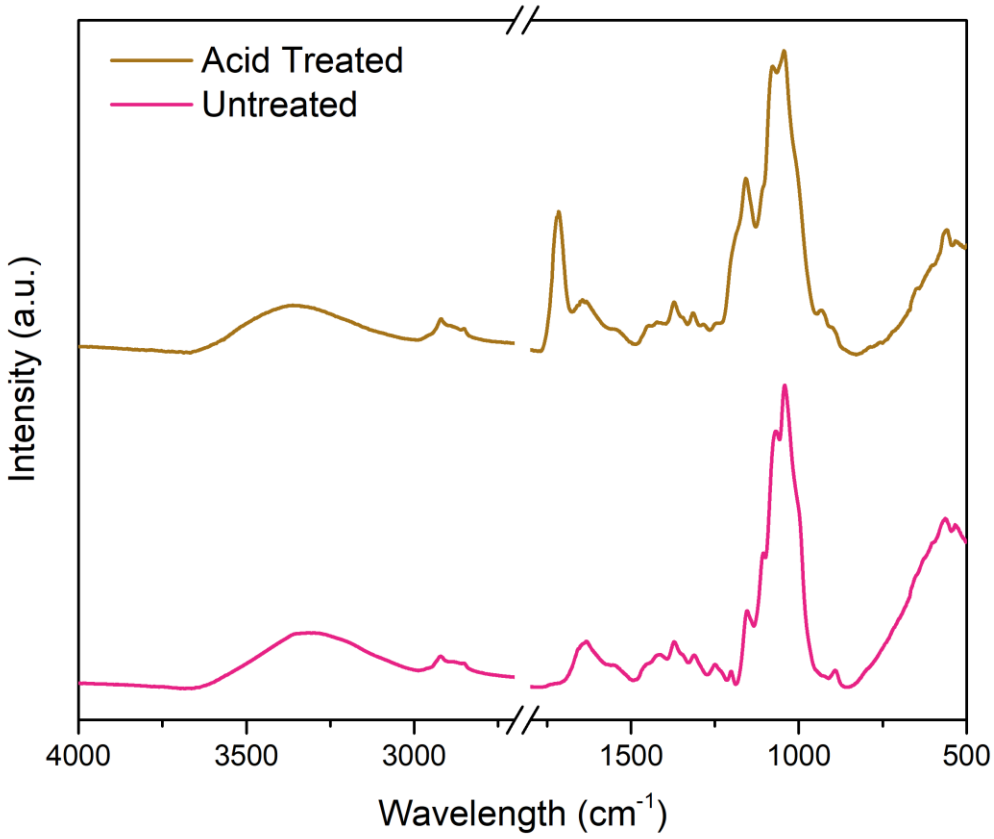

Figure S1. Full FTIR spectra of untreated and acid-treated MFilm

Table S1. Contact angle and moisture content comparison of *T.vers* MFilm and *T.vers* W/D MFilm

	***T.vers* MFilm**	***T.vers* W/D MFilm**
Contact angle (°)	126.4 (±5.6)	94.1 (±12.7)
Moisture content (%)	9.98 (±1.27)	9.84 (± 0.59)

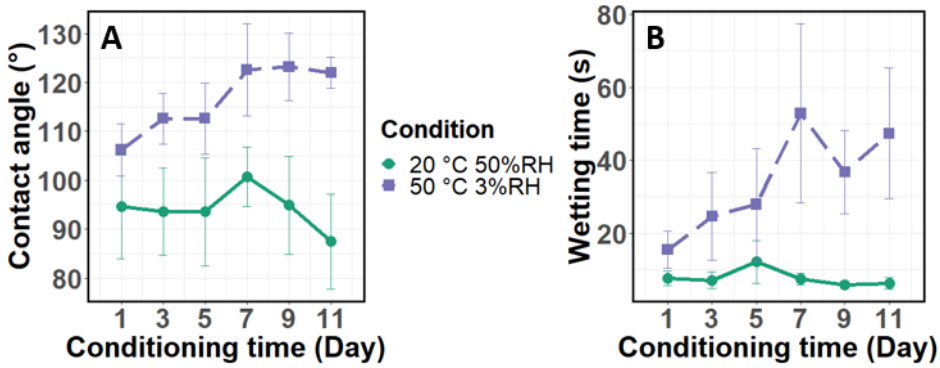

Figure S2. Change of contact angle (A) and wetting time (B) with conditioning time for *T.vers* W/D MFilm.

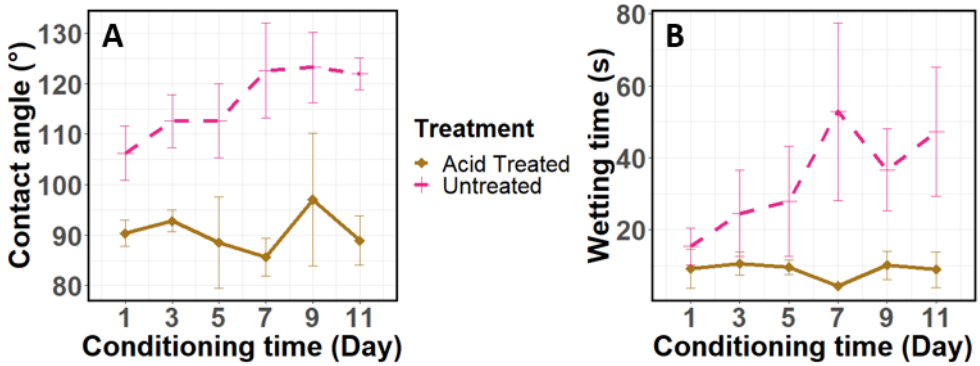

Figure S3. Influence of acid treatment on the contact angle (A) and wetting/absorption time (B) of *T.vers* W/D MFilm after different conditioning times (50 °C and 3%RH)

Experimental Section

Materials

Yellow birch (*Betula alleghaniensis* Britt.) wood veneers with a thickness of 0.61 (±0.04) mm were kindly supplied by Columbia Forest Products LLC (Presque Isle, ME, USA). *Trametes versicolor* (*T.vers*) was supplied by Ecovative Design LLC (Green Island, NY, USA) and had been maintained on agar plates at 4 °C and was pre-incubated on malt extract agar (MEA) plates before the incubation process.

Mycelium Incubation

The incubation methods were modified from the literature [1, 2]. Yellow birch veneers with the dimensions of 80 mm (length) × 80 mm (width) were steam sterilized (121 °C) for 60 min and soaked for about five seconds in 2% (w/v) corn steep liquor (CSL) (Sigma-Aldrich, Saint Louis, MO, USA) containing suspended fungal mycelium. One MEA plate overgrown by the fungus was mixed in 150 mL 2% (w/v) sterile CSL in a tissue grinder) before they were put in Petri dishes with MEA agar. Plastic canvas meshes were used as supports in between the veneer and agar. The Petri dishes were incubated at 28 °C, 80% relative humidity (RH) for 30 days.

REFERENCES

(1) Fackler, K.; Schmutzer, M.; Manoch, L.; Schwanninger, M.; Hinterstoisser, B.; Ters, T.; Messner, K.; Gradinger, C., Evaluation of the selectivity of white rot isolates using near infrared spectroscopic techniques. *Enzyme Microb. Technol.* **2007,** *41* (6-7), 881-887.
(2) Fackler, K.; Schwanninger, M.; Gradinger, C.; Hinterstoisser, B.; Messner, K. J. F. m. l., Qualitative and quantitative changes of beech wood degraded by wood-rotting basidiomycetes monitored by Fourier transform infrared spectroscopic methods and multivariate data analysis. **2007,** *271* (2), 162-169.